InGaN Laser Diodes-Gain, Spectra and Nonlinear Dynamics

Nahid Hassan[1] and Sazzad M.S. Imran[2]*

[1]*Dept. of Electrical and Electronic Engineering, University of Brahmanbaria, Bangladesh*

[2]*Dept. of Electrical and Electronic Engineering, University of Dhaka, Bangladesh*

**E-mail: sazzadmsi@du.ac.bd*

Received on 14 December 2022, Accepted for Publication 13 March 2023

ABSTRACT

In this era, short-wavelength laser diodes with quantum-well (QW) structures offer plenty of opportunities for improvement in laser performance and receive widespread attention. Therefore, we develop dynamic model of the violet-blue InGaN laser diodes (LDs) and discuss basic features of the device in this paper. We investigate longitudinal mode dynamics through detail numerical simulation of the rate equation model of the quantum-well LDs. We selectively observe several effects such as relaxation oscillation, mode competition, intensity noise etc. From the dynamic behavior of the gain spectrum and time-varying modal photon numbers we found that the higher intensity noise of the quantum-well structure was due to random fluctuation with time among the different modes. The results were explained considering the previously published findings to confirm the validity of the proposed rate equation model of the quantum-well structures.

Keywords: Device model, InGaN, intensity noise, mode competition, quantum noise, rate equation, semiconductor laser, violet-blue laser.

1. Introduction

InGaN semiconductor laser diodes have undergone through rapid improvements as of late [1-5] and offer several sought-after properties such as direct electric modulation, compact size, different spectral widths etc. Dynamics [6] and relaxation oscillation [7] effects in laser diodes are eminent and by employing the rate equation model that considers single longitudinal mode only, we may easily weigh these effects. In this paper, we use an improved simulation model considering multi-longitudinal modes in order to reproduce mode competition phenomena [8].

The behavior of electrons is firmly influenced by the quantum nature of the electron when the semiconductor microstructure is of nanometer size. These quantum structures have offered successful and alluring opportunities for improvement in semiconductor laser performances [9, 10]. For the first time Dingle *et al*. examined the optical features in quantum wells [11], since then the utilization of QW configurations in semiconductor lasers has received widespread consideration [12, 13] due to its remarkable aspects such as its lower threshold current density [14, 15], lower temperature dependency [16-18], notable dynamic properties [19-21] etc. K. Matsuoka *et al*. reports experimental data on quantum and feedback noise in InGaN QW semiconductor lasers and confirmed higher quantum noise compare to long-wavelength AlGaAs laser diodes [22]. Later, M. Ahmed presented a theoretical model of InGaN QW laser diodes that operates in single-mode and confirmed the above experimental findings through numerical simulation [23]. However, none of them could explain satisfactorily why we get aggravated noise properties in blue-violet lasers. After that, L. Uhlig *et al*. developed a multimode rate equation model of QW lasers and described their nonlinear dynamics [24]. However, L. Uhlig *et al*. didn't consider photon number fluctuation due to spontaneous emission.

In this article, we present an improved rate equation model of the violet-blue QW multimode InGaN LDs. In our model, we consider fluctuation in photon numbers due to spontaneous emission and two distinct quantum wells each having different carrier injection efficiency. The double-QW model can be easily extended to multiple quantum wells as well. Through exact numerical simulation of the rate equation model, we discuss basic features of the double-QW LDs with accentuation on its nonlinear dynamics and noise characteristics as well as properties of gain.

First, we introduce the improved rate equation model for the multimode double-QW InGaN laser diodes, and then through numerical simulation we discuss properties of the device. We also compare our simulation results with that of the other published findings to confirm the validity of our rate equation model.

2. Double-QW InGaN LD Model

M. Yamada *et al.* simulate dynamics of the InGaN lasers using the rate equation model in [25]. We have expanded the model to double-QW LDs in this paper. InGaN laser diodes typically have two to three quantum wells [26] and optimization of the number is a part of the development process [27]. Many have already observed unequal carrier injection into the multiple QWs [28, 29] and we consider the carrier densities are different in two different quantum wells to include this effect. We divide the total active area into two equal-sized parts and each part has been considered separately. In this scenario, carrier numbers corresponding to threshold, saturation and transparency are counting as half of the values for single QW. It is to mention that we can easily expand this model to three quantum wells. Also, the rate equation model is equally applicable to III-nitride LDs grown on c-plane, semipolar or nonpolar plan as we have considered dynamic effect of electron-hole concentration, electron lifetime and polarization field while deriving the

equations.

We can study nonlinear dynamics of the double-QW InGaN laser diodes by using the rate equations for the carrier number $N(t)$ and photon number $S_p(t)$ that can now be modified as follows.

$$\frac{dN_1}{dt} = -\sum_p A_{p1}S_p - \frac{N_1}{\tau_s} + \chi\frac{I}{e} \quad (1)$$

$$\frac{dN_2}{dt} = -\sum_p A_{p2}S_p - \frac{N_2}{\tau_s} + (1-\chi)\frac{I}{e} \quad (2)$$

$$\frac{dS_p}{dt} = \left(G_{p1} + G_{p2} - G_{th}\right)S_p + \frac{\xi a\,(N_1+N_2)/V}{\left(2\frac{\lambda_p-\lambda_0}{\delta\lambda}\right)^2+1} + F_{Sp}(t) \quad (3)$$

In the injection term in eqns. (1) and (2), carriers injected into the 1st QW is represented by χ and therefore the remaining (1-χ) carriers will go into the 2nd QW. Usually, the 1st QW is considered to be the stronger pumped one and therefore we consider the value of χ as $0.5 \geq \chi \leq 1$ [29]. N_1 and N_2 are the two different carrier numbers for the two different QWs. τ_s is the electron lifetime. To include unequal pumping, we define two linear modal gains for the two different quantum wells- for the 1st QW we consider A_{p1} as the linear gain of the p-th longitudinal mode and for the 2nd quantum well we consider A_{p2} as the linear gain term. G_{th} is the threshold gain of the LD active medium that corresponds to the sum of the internal loss k and the mirror loss due to front facet and back facet reflectivity R_f and R_b, respectively.

$$G_{th} = \frac{c}{n_r}\left[k + \frac{1}{2L}ln\frac{1}{R_fR_b}\right] \quad (4)$$

The modal gain G_p contains the linear gain term A_p, the self-saturation term $-BS_p$ and the mode coupling term. The last term is divided into symmetric D_{pq} and asymmetric H_{pq} parts [30]. Thus the expressions for G_{p1} and G_{p2} for the two different QWs are defined as

$$G_{p1} = A_{p1} - B_1S_p - \sum_{q\neq p}\left(D_{pq1} + H_{pq1}\right)S_q \quad (5)$$

$$G_{p2} = A_{p2} - B_2S_p - \sum_{q\neq p}\left(D_{pq2} + H_{pq2}\right)S_q \quad (6)$$

The coefficients A_{p1}, A_{p2}, B, D_{pq} and H_{pq} are defined as follows [31].

$$A_{p1} = \frac{a\xi}{V}\left[N_1 - N_g - bV\left(\lambda_p - \lambda_0\right)^2\right] \quad (7)$$

$$A_{p2} = \frac{a\xi}{V}\left[N_2 - N_g - bV\left(\lambda_p - \lambda_0\right)^2\right] \quad (8)$$

$$B_1 = \frac{9}{4}\frac{\hbar\omega_p}{\varepsilon_0 n_r^2}\left(\frac{\xi\tau_{in}}{\hbar V}\right)^2 aR_{cv}^2(N_1 - N_s) \quad (9)$$

$$B_2 = \frac{9}{4}\frac{\hbar\omega_p}{\varepsilon_0 n_r^2}\left(\frac{\xi\tau_{in}}{\hbar V}\right)^2 aR_{cv}^2(N_2 - N_s) \quad (10)$$

$$D_{pq1} = \frac{4}{3}\frac{B_1}{\left(\frac{2\pi c\tau_{in}}{\lambda_p^2}\right)^2\left(\lambda_p - \lambda_q\right)^2 + 1} \quad (11)$$

$$D_{pq2} = \frac{4}{3}\frac{B_2}{\left(\frac{2\pi c\tau_{in}}{\lambda_p^2}\right)^2\left(\lambda_p - \lambda_q\right)^2 + 1} \quad (12)$$

$$H_{pq1} = \frac{3}{8}\frac{\lambda_p^2}{\pi c}\left(\frac{a\xi}{V}\right)^2\frac{\alpha(N_1 - N_g)}{\lambda_q - \lambda_p} \quad (13)$$

$$H_{pq2} = \frac{3}{8}\frac{\lambda_p^2}{\pi c}\left(\frac{a\xi}{V}\right)^2\frac{\alpha(N_2 - N_g)}{\lambda_q - \lambda_p} \quad (14)$$

We assume that the mode p=0 has wavelength λ_0 and known as the central mode of the gain spectrum. The shift of wavelength due to thermal effect [32, 33] is neglected in the modal photon density calculation. Wavelengths of the other longitudinal modes can be written as

$$\lambda_p = \lambda_0 + p\Delta\lambda = \lambda_0 + p\frac{\lambda_0^2}{2n_rL} \quad p = 0, \pm1, \pm2, \ldots \quad (15)$$

Due to recombination and spontaneous emission, the photon number fluctuates. This fluctuation is introduced in eqn. (3) as function $F_S(t)$ that is known as Langevin noise source. We can approximate the function as Gaussian distribution with its mean value equal to zero and is given in the following equation.

$$F_{Sp}(t) = \sqrt{\frac{V_{SpSp}}{\Delta t}}.g_s \quad (16)$$

The variances V_{SpSp} in eqn. (16) is defined as-

$$V_{SpSp} = \left\{\frac{a\xi}{V}\left(N_1 + N_2 + N_g\right) + G_{th}\right\}S_p + \frac{a\xi}{V}(N_1 + N_2) \quad (17)$$

We generate random numbers through in the ranges between -1 and +1 [31, 34] and Δt is the small time-step considered in our calculation.

The noise contents in the time varying photon number fluctuation is determined in terms of the RIN (relative intensity noise). We calculate the RIN value from the temporal fluctuation $\delta S(t)=S(t)-S_{avg}$, where $S(t)=\sum S_p$ is the total photon number.

$$RIN = \frac{1}{S_{avg}^2}\left\{\frac{1}{T}\left|\int_0^T \delta S(\tau)\,e^{j\Omega\tau}d\tau\right|^2\right\} \quad (18)$$

where Ω is the Fourier frequency and S_{avg} is the time average photon number.

We then integrate the discrete version of the Eqn. (18) through fast Fourier transform and compute the values of the temporal intensity fluctuation as given in Eqn. (19).

$$RIN = \frac{1}{S_{avg}^2}\frac{\Delta t^2}{T}|FFT[\delta S(t_i)]|^2 \quad (19)$$

Optical power of the laser output can be calculated using the Eqn. (20) given below as

$$P(t) = \frac{(h\nu)c}{2n_rL}\frac{ln\left(1/R_fR_b\right)\left(1-R_f\right)}{\left(1-\sqrt{R_fR_b}\right)^2}\sum_p S_p \quad (20)$$

Here, $h\nu$ is the photon energy and c is the speed of light in vacuum.

3. Numerical Calculations

We investigate the behavior of the InGaN double-QW LDs through numerical simulation of the rate equation model

represented by the Eqns. (1)-(3). We have considered two distinct quantum wells with dissimilar pumping efficiency of the injected carriers. To solve the rate equations of the carrier and photon numbers, we use the Fourth-order Runge-Kutta method. We consider total 13 modes to simulate the rate equations that depict the multimode laser diode with peak wavelength $\lambda_0 = 410$ nm. We take a very short time step of $\Delta t = 5$ ps for the numerical simulation so that we can count on very high relaxation oscillation frequency. We also simulate the rate equation for at least 2 ms so that we can examine the laser output at a very lower frequency region. Values of the parameters of the InGaN laser diodes that were considered in our numerical simulation are given below [35-37].

Differential gain coefficient = $a = 1.85\times10^{-12}$ m^3/s, dispersion parameter of the linear gain spectrum = $b = 3\times10^{39}$ m^{-3}A^{-2}, half-width of spontaneous emission = $\Delta\lambda$ = 20 nm, dipole moment value = $R_{cv} = 1.22\times10^{-29}$ C^{2}m^2, linewidth enhancement factor = $\alpha = 2$, field-confinement factor = $\xi = 0.2$, unequal pumping parameter = $\chi = 0.7$, carrier intraband relaxation time = $\tau_{in} = 0.01$ fs, average carrier lifetime = $\tau_s = 2$ ns, electron number that characterizes nonlinear gain = $N_S = 2.01\times10^8$, transparent electron number = $N_g = 2.52\times10^8$, active region length of the LD = $L = 300$ μm, active region volume of the LD = $V = 100$ μm^3, active region refractive index of the LD = $n_r = 2.6$, internal loss in the LD cavity = $k = 5.2$ cm^{-1}, reflectivity of the LD front facet = $R_f = 0.4$ and reflectivity of the LD back facet = $R_b = 0.7$.

4. Results Analysis

Fig. 1 depicts the current vs. optical output power characteristics to show the static behavior of the laser diode. To understand its threshold behavior logarithmic value of optical power is also shown in the figure. From the continuous wave measurement, we get the slope efficiency as $dP/dI = 0.41$ W/A and the threshold current as $I_{th} = 27$ mA.

The self-saturation parameter B determines the effect of photon number currently presents in any single longitudinal mode on the gain of that particular mode. The value of B is same for all the longitudinal modes, but for the multi-QW laser diodes the impact of B is different in the different quantum wells because self-saturation parameter depends on the density of carrier presents in that particular quantum well and also takes into account the carrier saturation effect.

The mode cross-saturation has two parts- D_{pq} describes the symmetric part and H_{pq} describes the asymmetric part. The modal gain of neighboring modes is suppressed by the symmetric part of each mode and in the wavelength spectrum that part follows the Lorentz-distribution [24]. As the difference of wavelength between two coupling modes become larger, the effect of this interaction decreases. The asymmetric part is demonstrated as $(\lambda_q-\lambda_p)^{-1}$ in the rate equation model and thus the gain is higher for the neighboring modes in the longer wavelength direction and lower in the shorter wavelength direction.

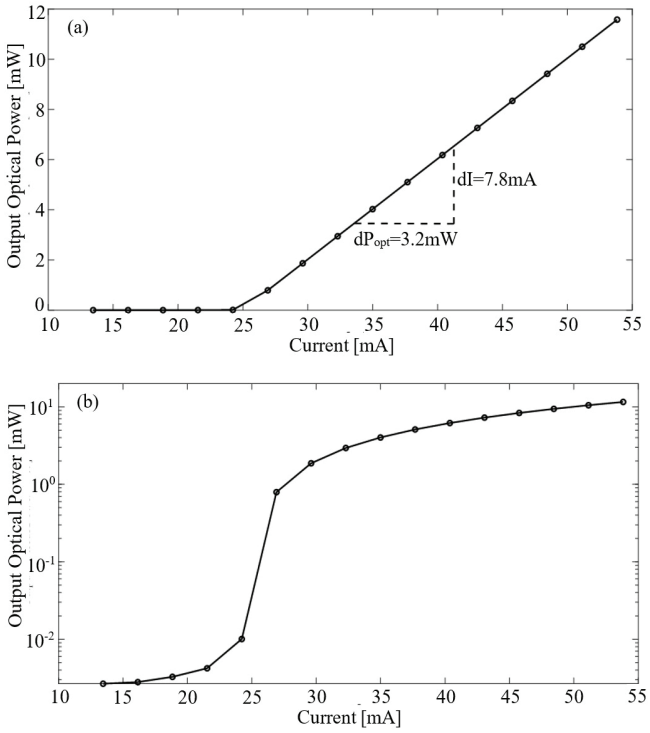

Fig. 1: Laser static characteristics. (a) Current vs. output optical power on a linear scale, the threshold current is calculated as 27 mA and the slope efficiency as 0.41 W/A. (b) Current vs. output optical power on a logarithmic scale to show the threshold behavior.

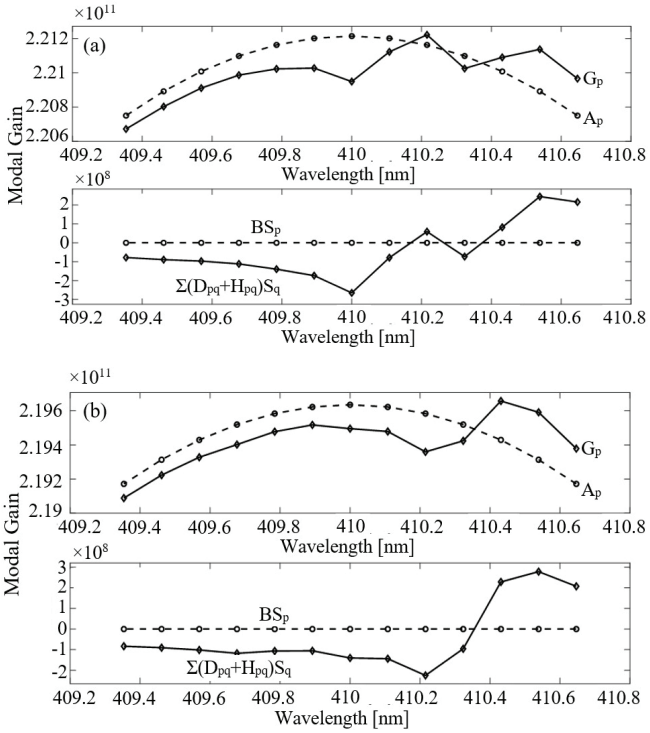

Fig. 2: Simulated gain spectrum at (a) $t = 30$ ns and (b) $t = 80$ ns, showing total gain and its linear term and self- and cross-saturation terms resulting from multimode simulation. This figure represents the gain characteristic at two different times and can be considered as a snapshot of its dynamic behavior.

The linear gain term A_p and modal gain G_p are shown in Fig. 2(a) together with the effect of self-saturation and cross-saturation parameters at time t = 30 ns and operating current $I = 1.8I_{th}$. However, that behavior is not static, rather time-dependent. To show its dynamic behavior we present the simulated gain spectrum at different time t = 80 ns in Fig. 2(b). The difference in the simulated modal gain at t = 30 ns and t = 80 ns may be attributed to a small wavelength drift due to the effect of ambient temperature, nonlinear current injection, or mechanical deformation of the cavity due to thermal expansion or mechanical stress in the laser cavity, resulting in a slight shift in the position of the resonant modes and a corresponding change in the modal gain at different wavelengths.

The dynamic behavior of the gain spectrum was confirmed by the temporal photon number fluctuation of the different modes shown in Fig. 3. The figure shows that the modal photon number fluctuates rather randomly and the dominant modes jump from one mode to another randomly with time. Also, the dominant modes shift towards the longer wavelengths due to the inverse effect of the asymmetric gain saturation term on the modal gain defined in Eqns (13) and (14). Due to this random fluctuation of the modal photon numbers, we get rather high relative intensity noise (RIN) in short-wavelength InGaN QW lasers compare to long-wavelength AlGaAs DH laser diodes. This properties were reported previously by K. Matsuoka *et al*. in [22] and M. Ahmed in [23]. M. Ahmed reported that 5 mW AlGaAs laser diode has LF-RIN value of around -150 dB/Hz whereas 5 mW InGaN laser diode has -135 dB/Hz. As mentioned in the Introduction, K. Matsuoka *et al*. presented their experimental findings and M. Ahmed their simulation results considering only the single-mode operation. Therefore, it was difficult for them to draw a conclusion for deteriorated noise properties of shorter wavelength lasers. From our multimode simulation, we can confirm that the higher RIN value of the InGaN QW lasers might be due to random fluctuation of the different longitudinal modes with time. It is to mention that, we get single-mode like operation with one dominant mode for AlGaAs DH lasers without external optical feedback as reported in [34].

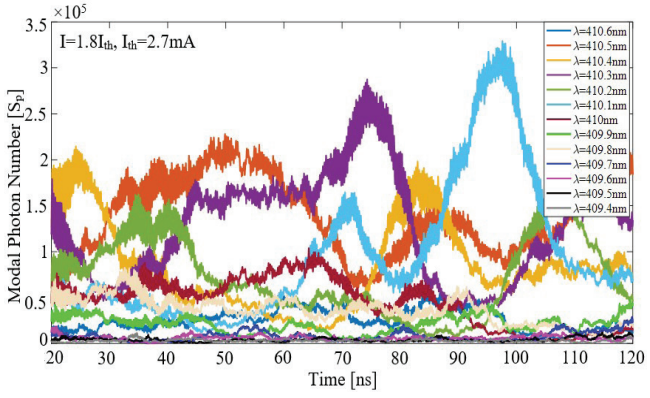

Fig. 3: Time variation of the photon number for all 13 dominant modes that we have considered in our numerical simulation.

We get total carrier number N by adding number of carriers in the two separate quantum wells and total photon number S by adding photon numbers of the all existing longitudinal modes. Temporal photon number variation and RIN properties of the 410 nm InGaN QW lasers are shown in Fig. 4. Total photon number fluctuates randomly around its time average value of S_{avg}=5.9×10^5. RIN characteristics show a peak at the relaxation oscillation frequency near 3.8 GHz.

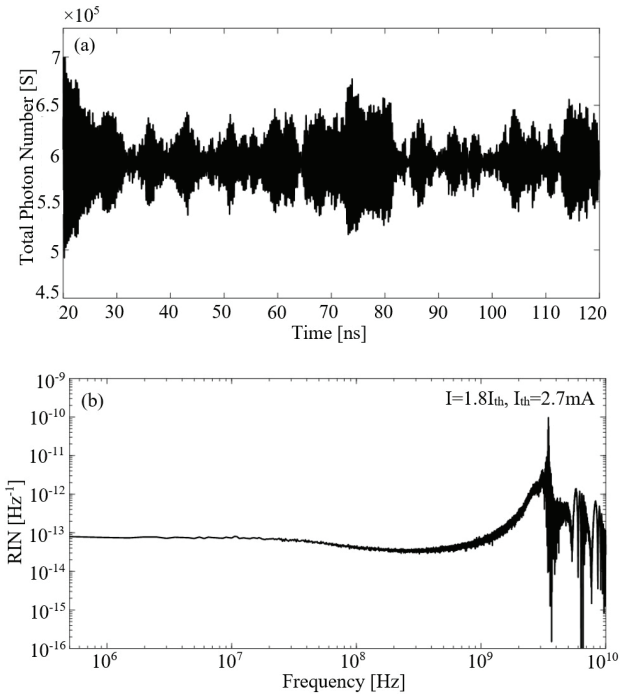

Fig. 4: (a) Time variation of total photon number at the laser output. (b) Quantum RIN characteristics of InGaN laser diodes at I=1.8I_{th}.

5. Conclusion

We have presented multimode rate equation model of the double-QW laser diodes considering different carrier injection efficiencies for different wells. Later, through numerical simulation of the rate equation model for the 410 nm InGaN lasers, we explain its dynamic properties of gain spectrum, RIN characteristics and mode competition phenomena.

In conclusion we can say, the 410 nm InGaN double-QW laser diodes may operate at higher threshold current and slope efficiency compare to long-wavelength laser diodes. Due to the effect of nonlinear and self- and cross-saturation gain terms, the dominant modes of laser diodes shift towards longer wavelength with time. Though the total photon number at laser output fluctuates around its average photon number, the optical signal jumps from one dominant mode to another rather randomly with time. Due to random fluctuation among several longitudinal modes with time, we get aggravated quantum RIN characteristics of the InGaN laser diodes compare to AlGaAs laser diodes.

Reference

1. D. Queren, A. Avramescu, G. Brüderl, A.Breidenassel, M. Schillgalies, S. Lutgen, and Unnnn bb. Straus, "500 nm electrically driven InGaN based laser diodes," *Appl. Phys. Lett.,* vol. 94, no. 8, 2009.
2. T. Miyoshi, S. Masui, T. Okada, T. Yanamoto,T. Kozaki, S.I. Nagahama, and T. Mukai, "510-515 nm InGaN-based green laser diodes on c-plane gan substrate," *Appl. Phys. Express,* vol. 2, 2009.
3. S.Lutgen, A. Avramescu, T. Lermer, D. Queren,J. Müller, G. Bruederl, and U. Strauss, "True green InGaN laser diodes," *Phys. Status Solidi A*, vol. 207, no. 6, pp. 1318-1322, 2010.
4. A. Avramescu, T. Lermer, J. Müller, C. Eichler,G.Brüderl, M. Sabathil, S. Lutgen, and U. Strauss, "True green laser diodes at 524 nm with 50 mW continuous wave output power on c-plane GaN," *Appl. Phys. Express*, vol. 3, no. 6, 2010.
5. H. König, M. Ali, W. Bergbauer, J. Brückner, G. Brüderl, C. Eichler, S. Gerhard, U. Heine, A. Lell, L. Naehle, M. Peter, J. Ristic, G. Rossbach, A. Somers, B. Stojetz, S. Tautz, J. Wagner, T. Wurm, U. Strauss, M. Baumann, A. Balck, and V. Krause, "Visible GaN laser diodes: from lowest thresholds to highest power levels," *Proc. SPIE 10939*, 2019.
6. L.A. Coldren, S.W. Corzine, and M.L. Mashanovitch, Diode Lasers and Photonic Integrated Circuits, *John Wiley & Sons, Inc.,* 2012.
7. K. Lüdge, M. J. Bormann, E. Malic, P. Hövel, M. Kuntz, D. Bimberg, A. Knorr, and E. Schöll, "Turn-on dynamics and modulation response in semiconductor quantum dot lasers," *Phys. Rev. B*, vol. 78, no. 3, 2008.
8. M. Yamada, "Theory of mode competition noise in semiconductor injection lasers", *IEEE J. of Quantum Electron.*, vol. 22, no. 7, pp. 1052-1059, 1986.
9. W. Tsang, "Heterostructure semiconductor laser's prepared by molecular beam epitaxy," *IEEE J. Quantum Electron.*, vol. QE-20, pp. 1119-1132, 1984.
10. P.S. Zory, Jr., Quantum Well Lasers, *Academic Press, New York,* 1993.
11. R. Dingle, A.C. Gossard, and W. Wiegmann, "Direct observation of super lattice formation in a semiconductor heterostructure", *Phys. Rev, Lett.*, vol. 34, pp. 1327-1330, 1975.
12. P. van der Ziel, R. Dingle, R.C. Miller, W. Wiegmann, and W.A. Nordland Jr., "Laser oscillation from quantum well states in very thin GaAl-A1GaAs multilayer structures," *Appl. Phys. Lett.,* vol. 26, pp. 463-465, 1975.
13. N. Holonyak, Jr., R. M. Kolbas, R. D. Dupuis, and P. D. Dapkus, "Quantum-well heterostructure lasers," *EEE J. Quantum Electron.*, pp. 170-181, 1980.
14. W.T. Tsang, "Extremely low threshold (A1Ga)As modified multiquantum well beterostructure lasers grown by molecular beam epitaxy," *Appl. Phys. Lett.*, vol. 39, pp. 786-788, 1981.
15. T. Fujji, S. Yamakoshi, K. Nanbu, 0. Wada, and S. Hiyamizu, "MBE growth of extremely high-quality GaAs-AIGaAs GRIN-SCH lasers with a superlattice buffer layer," *J. Vac. Sci. Technol.*, vol. 2, pp. 259-261, 1984.
16. R. Chin, N. Holonyak, Jr., B. A. Bojak, K. Hess, R. D. Dupuis, and P. D. Dapkus, "Temperature dependence of threshold current for quantum well AlGaAs-GaAs heterostructure laser diodes," *Appl. Phys. Lett.*, vol. 36, pp. 19-21, 1979.
17. K. Hess, B. A. Bojak, N. Holonyak, Jr., R. Chin, and P. D. Dapkus, "Temperature dependence of threshold current for a quantum-well heterostructure laser," *Solid-State Electron.*, vol. 23, pp. 585-589, 1980.
18. Y. Arakawa and H. Sakaki, "Multiquantum well laser and its temperature dependence of the threshold current," *Appl. Phys. Lett.*, vol. 45, pp. 950-952, 1984.
19. Y. Arakawa, K. Vahala, and A. Yariv, "Quantum noise and dynamics in quantum well and quantum wire lasers," *Appl. Phys. Lett.*, vol. 45, pp. 939-941, 1982.
20. Y. Arakawa, and A. Yariv, "Theory of gain, modulation response, and spectral linewidth in AlGaAs quantum well lasers," *IEEE J. Quantum Electron.*, vol. QE-21, pp. 1666-1674, 1985.
21. Y. Arakawa, K. Vahala, and A. Yariv, "Dynamic and spectral properties in semiconductor lasers with quantum well and wire effects," presented at the 2nd Int. Conf. Modulated Semiconductor Structures, *Kyoto, Japan*, 1985.
22. K. Matsuoka, K. Saeki, E. Teraoka, M. Yamada, Y. Kuwamura, "Quantum noise and feedback noise in blue-violet InGaN semiconductor lasers", *IEICE Trans. Electron.*, vol. E89-C, no. 3, 2006.
23. M. Ahmed, "Theoretical modeling of intensity noise in InGaN semiconductor lasers", *The Scientific World Journal*, vol. 2014, id 475423, pp. 1-6, 2014.
24. L. Uhlig, M. Wachs, D.J. Kunzmann, U.T. Schwarz, "Spectral-temporal dynamics of (Al,In)GaN laser diodes", *Optics Express*, vol. 28, no. 2, 2020.
25. M. Ahmed, M. Yamada, and M. Saito, "Numerical modeling of intensity and phase noise in semiconductor lasers," *IEEE J. Quantum Electron.*, vol. 37, no. 12, pp. 1600-1610, 2001.
26. K. Kojima, U. T. Schwarz, M. Funato, Y. Kawakami, S. Nagahama, and T. Mukai, "Optical gain spectra for near UV to aquamarine (Al, In)GaN laser diodes," *Opt. Express,* vol. 15, no. 12, pp. 7730-7736, 2007.
27. U. Straus, A. Avramescu, T. Lermer, D. Queren, A. Gomez-Iglesias, C. Eichler, J. Müller, G. Brüderl, and S. Lutgen, "Pros and cons of green InGaN laser on c-plane GaN," *Phys. Status Solidi B*, vol. 248, no. 3, pp. 652-657, 2011.
28. W. Scheibenzuber, "GaN-based laser diodes: Towards longer wavelengths and short pulses," *PhD Thesis, Universität Freiburg*, 2011.
29. W.G. Scheibenzuber and U.T. Schwarz, "Unequal pumping of quantum wells in GaN-based laser diodes," *Appl. Phys. Express,* vol. 5, no. 4, 2012.
30. M. Yamada, "Theoretical analysis of nonlinear optical phenomena taking into account the beating vibration of the electron density in semiconductor lasers," *J. Appl. Phys.*, vol. 66, no. 1, pp. 81-89, 1989.
31. S. Abdulrhmann, M. Ahmed, T. Okamoto, W. Ishimori and M. Yamada, "An improved analysis of semiconductor laser dynamics under strong optical feedback", *IEEE J. Selected Topics in Quantum Electron.*, vol. 9, pp. 1265-1274, 2003.
32. G. Ropars, A. Le Floch, and G. Agrawal, "Spectral and spatial dynamics in InGaN blue-violet lasers," *Appl. Phys. Lett.*, vol. 89, no. 24, 2006.
33. M.H. Chen, S.C. Hsiao, K.T. Shen, C.C. Tsai, and H.C. Chui, "The spectral mode evolution in a blue InGaN laser diode," *Optik*, vol. 186, pp. 41-45, 2019.

34. SMS Imran, M. Yamada, Y. Kuwamura, "A theoretical analysis of the optical feedback noise based on multimode model of semiconductor lasers", *IEEE J. Quantum Electron.*, vol. 48, pp. 521-527, 2012.

35. C. Lee, C. Zhang, D.L. Becerra *et. al.*, "Dynamic characteristics of 410 nm semipolar (2021) III-nitride laser diodes with a modulation bandwidth of over 5 GHz", *Appl. Phys. Lett.*, vol. 109, pp. 101104, 2016.

36. R.A. Abdullah, "The influence of gain suppression on dynamic characteristics of violet InGaN laser diodes", *Optik – International Journal for Light and Electron Optics*, vol. 125, no. 1, pp. 580-582, 2014.

37. Z. Zhang, J. Yang, D. Zhao, F. Liang, P. Chen and Z. Liu, "Theoretical Optical Output Power Improvement of InGaN-Based Violet Laser Diode Using AlGaN/GaN Composite Last Quantum Barrier", *Nanomaterials*, vol. 12, pp. 3990, 2022.